# Accepted Manuscript


Effects of noise-induced hearing loss on parvalbumin and perineuronal net expression in the mouse primary auditory cortex

Anna Nguyen, Haroun M. Khaleel, Khaleel A. Razak

PII: S0378-5955(17)30002-3

DOI: 10.1016/j.heares.2017.04.015

Reference: HEARES 7362

To appear in: *Hearing Research*

Received Date: 4 January 2017

Revised Date: 19 April 2017

Accepted Date: 24 April 2017

Please cite this article as: Nguyen, A., Khaleel, H.M., Razak, K.A., Effects of noise-induced hearing loss on parvalbumin and perineuronal net expression in the mouse primary auditory cortex, *Hearing Research* (2017), doi: 10.1016/j.heares.2017.04.015.

# Effects of noise-induced hearing loss on parvalbumin and perineuronal net expression in the mouse primary auditory cortex

Anna Nguyen[a], Haroun M Khaleel[b] and Khaleel A. Razak[b, c]

[a] Bioengineering Program, University of California, Riverside

[b] Psychology Department and Graduate Neuroscience Program, University of California, Riverside

[c] Corresponding author

Psychology Department

900 University Avenue

Riverside, CA – 92521

Email: khaleel@ucr.edu

Phone: 951-827-5060

Running title: Hearing loss and markers of cortical inhibition

Number of text pages: 27

Number of figures: 8

Number of tables: 0

**Abstract:**

Noise induced hearing loss is associated with increased excitability in the central auditory system but the cellular correlates of such changes remain to be characterized. Here we tested the hypothesis that noise-induced hearing loss causes deterioration of perineuronal nets (PNNs) in the auditory cortex of mice. PNNs are specialized extracellular matrix components that commonly enwrap cortical parvalbumin (PV) containing GABAergic interneurons. Compared to somatosensory and visual cortex, relatively less is known about PV/PNN expression patterns in the primary auditory cortex (A1). Whether changes to cortical PNNs follow acoustic trauma remains unclear. The first aim of this study was to characterize PV/PNN expression in A1 of adult mice. PNNs increase excitability of PV+ inhibitory neurons and confer protection to these neurons against oxidative stress. Decreased PV/PNN expression may therefore lead to a reduction in cortical inhibition. The second aim of this study was to examine PV/PNN expression in superficial (I-IV) and deep cortical layers (V-VI) following noise trauma. Exposing mice to loud noise caused an increase in hearing threshold that lasted at least 30 days. PV and PNN expression in A1 was analyzed at 1, 10 and 30 days following the exposure. No significant changes were observed in the density of PV+, PNN+, or PV/PNN co-localized cells following hearing loss. However, a significant layer- and cell type-specific decrease in PNN intensity was seen following hearing loss. Some changes were present even at 1 day following noise exposure. Attenuation of PNN may contribute to changes in excitability in cortex following noise trauma. The regulation of PNN may open up a temporal window for altered excitability in the adult brain that is then stabilized at a new and potentially pathological level such as in tinnitus.

Keywords: hearing loss, auditory cortex, parvalbumin, extracellular matrix, perineuronal nets, interneurons, inhibition

## 1. Introduction:

Even relatively brief exposure to loud noise can cause hearing loss or threshold shifts. Such noise-induced threshold shifts remain a common, but preventable, hearing disorder. Noise exposure may also lead to the development of tinnitus and hyperacusis (Roberts et al., 2010). Several lines of evidence suggest that noise exposure increases excitability in the central auditory system perhaps as a consequence of damage to cochlear hair cells and the resulting reduction in afferent input. This compensatory increase in gain manifests across the auditory neuraxis and occurs over multiple and overlapping temporal trajectories suggesting complex underlying mechanisms (Syka et al., 1994; Syka and Rybalko, 2000; Yang et al., 2011, 2012; Pilati et al., 2012; Berger and Coomber, 2015; Luo et al., 2016; reviewed in Wang et al., 2011 and Eggermont 2015). The cellular correlates of these changes in excitability are not well characterized.

One prominent hypothesis for noise-induced increase in excitability in the primary auditory cortex (A1) is reduced inhibition (Syka and Rybaldo, 2000; Yang et al., 2011; Llano et al., 2012). While physiological studies have characterized synaptic inhibition and how inhibition changes following noise exposure, the cellular substrates that are altered are only beginning to be understood (Scholl and Wehr, 2008; Novak et al., 2016). Inhibitory interneurons in sensory cortices can be classified based on co-expression of various markers and physiological response properties. Novak et al. (2016) showed that cortical somatostatin and parvalbumin-expressing (PV+) interneurons show relatively fast and layer-specific changes in activity following noise

72 trauma potentially leading to increased gain. Whether changes in responses of these cells are
73 associated with circuit level or intrinsic factors remain unclear.

74 The present study focused on perineuronal nets (PNN), a cellular structure commonly
75 found around GABAergic cells (reviewed in Takesian and Hensch, 2013). PNNs are specialized
76 extracellular matrix components that consist of chondroitin sulfate proteoglycans (CSPG). These
77 CSPGs are found throughout the extracellular matrix, but are highly dense around cortical PV+
78 inhibitory interneurons (McRae et al., 2007). While PV/PNN expression has been well studied in
79 somatosensory and visual cortex of rodents, focus on A1 is relatively recent and sparse (Happel
80 et al., 2014; Fader et al., 2016; Brewton et al., 2016; reviewed in Sonntag et al., 2015). PNNs are
81 involved with developmental and adult plasticity (Happel et al., 2014; Nakamura et al., 2009;
82 Pizzorusso et al., 2002) and provide protection against oxidative stress for PV+ cells (Cabungcal
83 et al., 2013). These data suggest that changes in PNN expression following acoustic trauma may
84 contribute to cortical plasticity leading to increased excitability. A loss of PNNs may decrease
85 excitability of PV+ interneurons and thus reduce inhibition in the cortical circuit (Balmer, 2016).
86 Therefore, the main aim of this study was to quantify cortical PNN expression following acoustic
87 trauma that induces persistent threshold shifts. We report here that noise exposure does not
88 change the density of PV+, PNN+ or PV/PNN co-localized cells. However, PNN intensity is
89 reduced in a cortical layer-and cell-type specific manner. The effect of trauma on PNN intensity
90 appears to be relatively more severe on PNN cells that do not express PV. Some changes are
91 seen even at the earliest examined time point (1 day post-exposure). These data suggest that
92 altered PNN properties may be at least one of the cellular mechanisms involved in enhanced
93 excitability of cortical neurons following acoustic trauma.
94

## 2. Material and methods

### *2.1. Animals*

All animal procedures were approved by the University of California, Riverside Institution Animal Use and Care Committee. Female CBA/CaJ mice at 4 weeks old were received from Jackson Laboratory and housed at a 12:12 light/dark cycle. Standard lab chow and water were given *ad libitum*. All animals were housed in the same room except for the noise exposure and auditory brainstem response (ABR) measurements. Each of the four groups (control and 1, 10, and 30 days post-exposure) consisted of n=5 mice.

### *2.2. Noise-Induced Hearing Loss Paradigm*

Noise exposure was done in a sound-attenuating booth (Gretch-Ken, OR). Mice were placed in a standard cage and were able to freely move during the duration of the exposure to noise. A Fostex 96TX speaker was placed facing down on top of the cage's lid. The sound stimulus used was a 102-104 dB SPL, narrowband noise (6-12 kHz) for 8 hours. No food or water was provided during the duration of the exposure to noise. The control mice spent the same amount of time in the sound-attenuating booth, but did not receive noise exposure.

### *2.3. Auditory Brainstem Response (ABR)*

Animals were anesthetized with isoflurane inhalation for the duration of the ABR procedure at a concentration of 0.5-0.75% in air. Three platinum coated electrodes were placed under the dermis of the head: the recording electrode was on the vertex, the ground electrode was in the left cheek and the reference electrode was in the right cheek. The sound stimuli were delivered via a free field speaker (MR1 Multi-Field Magnetic Speakers, Tucker-Davis Technologies) that

was placed 10 cm away from the left ear at 45 degrees. Clicks of alternating ±1.4 volts (duration 0.1 ms) were generated and delivered using RZ6 hardware (Tucker-Davis Technologies, FL). Intensity of the clicks ranged from 10-90 dB in 10 dB steps. The goal of the ABR measurement was to determine if threshold shifts occurred following noise exposure and to ensure that such shifts lasted at least 30 days. The goal was not to identify precise frequency-specific hearing levels over the course of the experiments. Therefore, clicks with a sound level resolution of 10 dB steps were used for threshold measures. The ABRs were filtered and amplified (Grass Technologies) and averaged (BioSigRZ, Tucker-Davis Technologies) before analysis. The ABR measurements were made on all mice before exposure to noise and after the noise exposure at 1 day, 10 days and 30 days post-exposure (PE). ABRs from control mice were also measured at the same four time points referenced to when they were placed in the sound booth without noise exposure.

*2.4. Immunohistochemistry and Image Analysis*

Mice were overdosed with sodium pentobarbital (i.p. 125 mg/kg) and perfused transcardially with cold solutions of 0.1 M phosphate buffered saline (PBS) (pH = 7.4) followed by 4% paraformaldehyde (PFA) (pH=7.4). Mice were perfused for each time point (1, 10, and 30 days) post-exposure (PE) to noise. The control mice were perfused along with the 30-day PE mice. The brains were extracted from the skull and post-fixed at 20°C in 4% PFA for 2 hours before storage in 0.1 M PBS with sodium azide. Brain tissues were sunk in 30% sucrose for 24-48 hours and coronal sections of 40 µm thickness were cut with a cryostat (CM 1860, Leica Biosystems). Three to six sections containing A1 were stained and analyzed per mouse. The distance between the sections was between 40-480 µm. It is possible that there is differential penetration of PV

and WFA antibody in the 40 µm thick sections. However, because our main aim was to determine how noise exposure alters PV/PNN expression, the comparison across experimental groups is unlikely to be influenced by differential antibody penetration. All immunohistochemistry was done on a shaker at room temperature unless stated otherwise. Free floating sections were washed at room temperature with 0.1M PBS 2x for 15 minutes then quenched with 50mM of $NH_4Cl$ for 15 minutes and then washed with 0.1M PBS 3x for 10 minutes. Next, the sections were permeablized with 0.1% triton-x for 10 minutes. Sections incubated in blocking solution consisting of 5% normal goat serum (NGS) and 1% bovine serum albumin (BSA; Fisher BioReagents Bovine Serum Albumin, Fraction V, Cold-ethanol Precipitated; BP1605-100) in 0.1M PBS for 1 hour. The sections were then incubated overnight at 20° C in 1% NGS, 0.5% BSA 0.1% Tween-20, 1:500 agglutinin *Wisteria floribunda* (fluorescein conjugated, FL-1351, Vector Laboratories) and 1:5000 rabbit anti-parvalbumin (PV-25, Swant). Sections were washed with 0.5% Tween-20 3x for 10 minutes and incubated in secondary antibody solution consisted of 1:500 donkey anti-rabbit 647 (A-31573, Life Technologies) in 0.1M PBS. The sections were then washed with 0.5% Tween-20 2x for 10 minutes and with 0.1M PBS for 10 minutes, mounted on a glass slide and allowed to air dry. The slides were cover-slipped with the mounting medium, Vectashield containing DAPI (Vector Laboratories), and the edges of the coverslip were sealed (Cytoseal 60, Richard-Allan Scientific).

The location of A1 was identified as previously described by Martin del Campo, et al., (2012). In this previous study, electrophysiological mapping was used to identify tonotopy in both A1 and anterior auditory field (AAF). The boundary between A1 and AAF was identified using the reversal of tonotopy (Trujillo et al., 2011) and was marked with a dye. Coronal sections with the identified boundary were compared with sections in Paxinos mouse brain atlas.

This provided the landmarks (primarily hippocampal shape) to identify A1 sections used in the present study. One challenge is that the reversal of tonotopy from A1 to AAF is not sharp. Therefore, it is possible that some of the sections analyzed include AAF. However, identical landmarks were used across experimental groups and all analyses were done blind to the experimental group.

Sections containing A1 were imaged using a confocal microscope (TCS SP5, Leica Microsystems) at 20x. The number of PV and PNN cells from summed z-stacks were counted in A1 from a 400 µm wide area across layers I-VI. The area from the pia to 50% of the cortical depth was defined as layers I-IV and from 50% depth to the white matter was defined as layer V-VI (Anderson et al., 2009). We were unable to differentiate layers more specifically because the layer boundary between layers III and IV or between V and VI cannot be distinguished with accuracy using Nissl stains. Images of PV and PNN were encoded and an experimenter blinded to the identity of the groups performed the cell counts. PNN cells were manually identified by discernible WFA staining that is circular with a hollow center. PV cells were manually identified based on the shape and size of staining. There was very little background PV staining with this protocol, facilitating identification of cells. Only cell bodies that were fully within the borders of the counting window were included in the tally.

*2.5. Data Analysis*

Three aspects of PV/PNN expression were compared across the four groups (control, 1, 10 and 30 day post exposure): the density of PV/PNN expression, the overall PNN intensity across the 6 layers and the PNN intensity around cells. Cell counts and intensity measurements were obtained with ImageJ software (NIH). The number of PV+, PNN+, and co-localized (PV/PNN)

cells were counted across all 6 cortical layers. The total area of the cortex was then used to calculate cell densities (cells/$mm^2$) of each cell type.

Deterioration of PNN intensity following enzymatic PNN degradation can result in reduced excitability of PV+ neurons (Balmer 2016). The effects of PNN deterioration may occur even without a loss of PNN+ cell density (Enwright et al., 2016). Therefore, we quantified PNN intensity following acoustic trauma. To determine the PNN intensity, a rectangle (width of 400 µm and depth extending from pia to bottom of layer VI) was first drawn on the image of the cortical section (e.g., Figure 2A, B). The average PNN intensity within the rectangle was determined as the average of all pixel intensity value in the PNN color channel. The background intensity was subtracted from each image for PNN intensity analysis. Background was defined as the average pixel intensity of a 40 x 40 µm area in layer 1 where there is very little PNN (Brewton et al., 2016).

We also analyzed PNN intensity in the region around individual PNN cells. For this cellular PNN intensity analysis, 30% of the PNNs in each imaged A1 section were randomly (random number generator) selected. If 30% was less than 12 PNN cells, then a minimum of 12 cells was analyzed. A 40 µm (66 pixels) horizontal line was drawn across the middle of the PNN surrounding each analyzed cell. The pixel intensity was plotted as a function of distance along this line. This resulted in a bimodal peaked plot (e.g., Figure 7) with the two peaks corresponding to the locations where the line intersected the most intense part of the PNN ring structure on both sides of the cell. The area under the curve for each PNN analyzed was averaged within each image. The specific statistical tests used are reported in the results section below.

**Results:**

*3.1. Noise Exposure Causes Persistent Threshold Shift*

ABR measurement before and after noise exposure was used to quantify hearing threshold shifts. ABR measurements were made in response to clicks of 0.1 ms duration with intensities of 10-90 dB in 10 dB steps. The threshold was the lowest sound level at which at least 1 peak was discernible within 7 msec from sound onset. In the example series of ABR plots from a control mouse (Figure 1A), the threshold was between 30-40 dB SPL. The noise-exposed mouse (Figure 1B) had a hearing threshold >90 dB SPL (the highest level tested in this study). The thresholds before noise exposure across all the mice in this study were in the 30-50 dB SPL range, consistent with previous ABR measurements in the mouse (Zhou, 2006). Change in threshold following noise exposure was quantified at 1 day (n=5 mice), 10 days (n=5 mice) and 30 days (n=5 mice) after exposure. The control mice (n=5) also had their ABRs measured at each of the same time points. The thresholds, except for one mouse, were fairly constant in the control mice across multiple days (Figure 1C). Even in the mouse that showed increased variability across days, the threshold never exceeded 50 dB SPL. Noise exposure caused an increase in threshold to >90 dB SPL at all three PE time points (Figure 1D-F) indicating that hearing loss lasted at least 30 days PE in the noise exposed mice.

FIGURE 1 AROUND HERE.

### *3.2 Expression of PV and PNN in the Mouse A1*

Parvalbumin and PNN expression in A1 was quantified in control and noise-exposed mice. Figure 2A shows a photomicrograph of a coronal section through A1 from a control mouse. The area within the white rectangle is reproduced in Figure 2B and shows the window within which the various measurements were made in this image. Figure 2C, D, E show example PV+, PNN+ and PV/PNN co-localized neuron, respectively (arrows in Figure 2B). Qualitative observations indicate that PV and PNN staining was essentially absent in layer I while layer II contains PV cells, but very little PNN. Consistent with Brewton et al., (2016), PNN was concentrated in layers IV-VI of A1, particularly in layer IV in which a band of cellular and neuropil staining was seen (Figure 2B). Figure 3 shows example photomicrographs obtained from PE mouse cortex. Qualitatively the distribution of cell types in the PE mice was similar to control A1.

Quantification of control and PE cell density data are shown in Figure 4. In control A1, there were more PNN+ cells than PV+ cells (paired two-tail t-test, $t(df) = 5.925$ $p < 0.0001$, $R^2=0.5563$). This was true in both superficial (I-IV) and deep (V-VI) layers. A strong association between PV and PNN cells has been reported in several brain regions (Sonntag et al., 2015). Therefore, the percentage of PV+ cells that was enwrapped by PNN was calculated in A1. Approximately 46% (± 0.0215 s.e.) of PV+ cells also expressed PNN in control A1. There was no difference in the percentage of PV/PNN co-localized cells between the deep and superficial layers in control A1 (paired two-tail t-test, $t(df) = 0.31$, $p = 0.75$, $R^2 = 0.003$). These data provide baseline quantification of PV/PNN expression in A1 in the control adult CBA/CaJ mice.

256 FIGURE 2 AROUND HERE.

257

258 Persistent threshold shift does not alter the density of PV+ and PNN+ cells in A1 after
259 noise induced hearing loss. There were no significant differences between groups in layers I-VI
260 for PV+ (1-way ANOVA, $F(3,119) = 1.06$, $p=0.37$), PNN+ (1-way ANOVA, $F(3,119) = 2.57$, $p$
261 $= 0.08$) or PV/PNN co-localized (1-way ANOVA $F(3,119) = 0.59$, $p = 0.63$) cell densities.
262 There were no differences in the density of PV+ cells in either layers I-IV or V-VI (1-way
263 ANOVA, $F(3,119) = 0.89$, $p = 0.45$, $F(3,119) = 0.87$, $p = 0.46$, respectively). There were no
264 significant differences in PNN+ cell density in layers I-IV (1-way ANOVA,
265 $F(3,119)=1.178$,$p=0.3211$). A trend was seen for PNN+ cell density to be reduced in layers V-
266 VI following noise exposure (1-way ANOVA, $F(3,119)=2.696$, $p=0.05$). The decrease in PNN+
267 cells density in layers I-VI ($p=0.08$), and specifically in layers V-VI ($p=0.05$) approach statistical
268 significance. However, we interpret these data conservatively as no significant difference with
269 the acknowledgement that a moderate risk for type II error may be present in this interpretation.
270 There were no significant differences in PV/PNN co-localized cell density in layers I-IV or V-VI
271 (1-way ANOVA, $F(3,119)=0.5178$, $p=0.6708$, $F(3,119)=0.5796$, $p=0.6295$, respectively). There
272 was also no significant differences in the percentage of PV+ cells that co-expressed PNN
273 between the different groups (1-way ANOVA, $F(3,119)=2.063$, $p=0.1088$) .

274

275 FIGURE 3 AROUND HERE.

276 FIGURE 4 AROUND HERE.

277

Previous studies suggest that a decline in PNN intensity may reflect changes in PNN organization. This change in PNN intensity may occur independent of changes in PNN+ cell density (Carulli et al., 2010; Balmer 2016; Enwright et al., 2016). Therefore, we compared A1 PNN intensity between control and PE mice. Example photomicrographs of PNN are shown in Figure 5. First, the average pixel intensity across the entire rectangle (400 µm wide, pia to bottom of layer VI depth) was determined. A significant decrease in the average pixel intensity of PNN across A1 was seen following acoustic trauma (2-way ANOVA, main effect of Layer $F(1,226)=10.18, p=0.0016$, main effect of Group $F(3,226)=9.9338$, $p<0.0001$, interaction of Group x Layers $F(3,226)=2.168$, $p= 0.0927$). When considering all 6 layers together, a significant decrease in PNN pixel intensity was observed at 1 and 10 day PE (1-way ANOVA, $F(3,230)=8.835$, $p<0.0001$, $R^2=0.1033$ with Bonferroni post-hoc Control vs 1 Day PE $p<0.001$, Control vs 10 Day PE $p<0.001$, 10 Days PE vs. 30 Days PE, $p<0.05$; other pairs, $p>0.05$) (Figure 6A). This indicates a decrease in PNN intensity even at 1 day PE. Interestingly, at day 30 PE, the intensity was similar to control levels suggesting a recovery. Layer-specific analysis shows that layer I-IV shows a decline in PNN intensity at each PE time point with no recovery (1-way ANOVA, $p=0.0001$, Bonferroni tests: Control vs. 1 Day PE, $p<0.001$; Control vs. 10 Days PE, $p<0.01$; Control vs. 30 Days PE; $p<0.05$, other pairs, $p>0.05$)). Layer V-VI shows a declining in PNN intensity only at 10 day PE with recovery at 30 day PE (1-way ANOVA, $F(3,113) = 4.623$, $p = 0.004$, Bonferroni tests: Control vs. 10 Days PE, $p < 0.05$; 10 Days PE vs. 30 Days PE; $p < 0.05$, other pairs, $p > 0.05$). Thus, the return of PNN intensity to control levels may be carried by changes in the deeper layers. Together these data indicate a relatively rapid and layer-specific decrease in PNN intensity in A1 following noise induced hearing loss.

FIGURE 5 AROUND HERE.

FIGURE 6 AROUND HERE.

While the above analysis provides information about PNNs across the entire depth of A1, studies of epileptogenesis and songbird brain development (Dityatev et al., 2007; Balmer et al., 2009) have suggested the integrity of PNN around the cell may provide additional markers of changes to PNN with functional consequences. Therefore, we analyzed PNN intensity in the region around individual cells. Figure 7 shows examples of how such measurements were made. A 40 µm line was centered on the PNN and the pixel intensity along this line was measured. The two peaks correspond to the regions of maximum cellular PNN intensity. The area under the curve was measured for 30% of randomly selected PNN+ cells, averaged across cells and compared across treatment conditions.

The PNN intensity around cells in layers I-VI declined significantly following noise induced hearing loss (Figure 8A). The decline was significant at 10 and 30 days PE exposure (1-way ANOVA $F(3,400)=8.753, p<0.0001, R^2=0.0616$, Bonferroni post-hoc: Control vs 10 Days PE, $P<0.001$, Control vs 30 Days PE $P<0.05$). Layer specific analysis indicates that there was a decline in layers I-IV that was significant at all PE days (1-way ANOVA $F(3,204)=6.402, p=0.0004, R^2=0.08605$ with Bonferroni post-hoc: Control vs 1 Day PE $P<0.05$, Control vs 10 Days PE $P<0.01$, Control vs 30 Days PE $P<0.001$) (Figure 8B). For layers V-VI cells, PNN intensity showed a significant decline only at 30 days PE (1-way ANOVA $F(3,192)=3.778$, $p=0.001$, $R^2=0.078$ with Bonferroni post-hoc: Control vs 30 Days PE $p<0.05$, all other pairs $p>0.05$) (Figure 8B, C). There was no significant interaction between groups and layers (two-way ANOVA $F(3,396)=2.18$, $p=0.09$).

FIGURE 7 AROUND HERE.

FIGURE 8 AROUND HERE.

The cellular analysis method also allows examination of whether PNN intensity changes are cell-type specific. Here we examined if PV/PNN co-localized cells were more or less susceptible to noise exposure compared to PNN+ cells that did not have PV (Figure 8C). For the PV/PNN co-localized cells, a significant effect of noise exposure was observed only at 30 day PE (1-way ANOVA $F(3,191)=3.778$, $p=0.0115$, $R^2=0.05601$ with Bonferroni post-hoc: Control vs 30 Days PE, $p<0.05$, all others $p>0.05$), whereas the PNN cells without PV showed significantly attenuated intensity at both 10 and 30 days PE (1-way ANOVA $F(3,205)=5.930$, $p=0.0007$, $R^2=0.0799$ with Bonferroni post-hoc: Control vs 1 Day PE, $P>0.05$, Control vs 10 Days PE, $P<0.01$, Control vs 30 Days PE, $p<0.01$). There was no significant interaction between group and cell type (2-way ANOVA interaction of Group x Cell Type $F(3,396)=0.59$, $p=0.62$).

*3.3. Additional Analyses*

The previous analyses used individual sections as independent samples because the sections likely covered different isofrequency contours in A1. A second analysis was performed by averaging data from all sections from each mouse and using the animal number as sample size. Although this analysis is underpowered (n=5 mice per group), the interpretation that PNN intensity declines after noise exposure was supported. One-way ANOVA showed a significant decline in overall PNN intensity across layers I-VI (Figure 6A) following noise exposure ($F(3,16) = 3.3$, $P<0.05$) with post-hoc comparison showing a significant difference between control

and 10 Days PE ($P<0.05$). Layer-specific analyses reveals superficial layers to be more impacted than deep layers. In layer I-IV, overall PNN intensity (Figure 6B) declined following noise exposure (one-way ANOVA, $F(3,16) = 3.24$, $P<0.05$) with post-hoc comparison showing all three noise exposure groups significantly different than control. In layer V-VI, however, there was no difference (one-way ANOVA, $F(3,16)=1.63$, $P>0.5$). When cellular PNN intensities were considered (Figure 8), there was a trend when all six layers were considered (one-way ANOVA, $F(3,16=2.6$, $P=0.08)$). Cellular PNN intensity showed a strong trend towards exposure-related decline in both layers I-IV (one-way ANOVA, $F(3,16)=2.87$, $P=0.06$) and V-VI (one-way ANOVA, $F(3,16)=2.97$, $P=0.06$) with the control mice different than 10 and 30 days post exposure mice ($P<0.05$). Taken together, these data show that PNN intensity in auditory cortex declines following noise exposure.

**3. Discussion:**

This study quantified the distribution of PV/PNN staining in primary auditory cortex of adult CBA strain mice, a commonly used strain to study auditory processing. We quantified the effects of persistent hearing threshold shifts on the expression of PV/PNN in A1. Consistent with previous studies of the auditory cortex (Brewton et al., 2016; Happel et al., 2014), approximately 45% of PV+ neurons in A1 are wrapped by PNNs. We tested the hypothesis that noise induced hearing loss will cause a deterioration of PNN. We show that the density of PV/PNN expressing cells does not change up to at least 30 days PE, but the intensity of PNN staining across the cortical depth and in regions around individual cells shows a relatively rapid decline following acoustic trauma. These data have implications for involvement of cell-type specific changes in A1 following acoustic trauma that may lead to increased gain.

370

371 4.1. PV/PNN Expression in the Primary Auditory Cortex

372 Although the expression of PNN and its association with specific cell types have been
373 well characterized in rodent visual and somatosensory cortex (Pizzorusso et al., 2002; McRae et
374 al., 2007; Takesian and Hensch, 2013; Liu et al., 2013) and subcortical auditory areas (Beebe et
375 al., 2016), the expression pattern in A1 has only recently been studied (Happel et al., 2014;
376 Brewton et al., 2016, reviewed in Sontagg et al., 2015). There is a higher density of PNN cells in
377 layers IV-VI with a band like appearance of cellular and neuropil staining in layer IV. These
378 data are consistent with observations made in rodent primary sensory cortices including A1
379 (Brückner et al., 1994; Happel et al., 2014; Fader et al., 2016; Brewton et al., 2016). The density
380 of PNN reported here is larger than that reported by Fader et al., (2016) and Brewton et al.,
381 (2016), but is similar to that reported by Happel et al., (2014). These differences may arise due
382 to strain differences and/or thresholds used for counting PNN. The density of PV+ cells is
383 similar to previous reports of mouse A1 (Martin del Campo et al., 2012). The relatively strong
384 association of PV and PNN (~45% of PV+ cells express PNN) in A1 is consistent with
385 observations made in other brain regions (Kosaka and Heizmann, 1989; Celio et al., 1993;
386 Pantazopoulos et al., 2006; Liu et al., 2013; Yamada et al., 2014). The observation that a
387 significant percent of PV+ cells were not covered by PNN and that PNN covered many cells that
388 did not express PV indicate the need for future studies of A1 to identify the distribution of
389 various cells types with PNN.

390

391 4.2. Effect of Hearing Loss on PV/PNN Expression

The main aim of the study was to determine if acoustic trauma that produces long lasting increase in hearing threshold affected expression of PV/PNN in A1. The noise exposure method used in this study effectively increased hearing thresholds from <50 dB SPL pre-exposure to >90 dB SPL post-exposure. This hearing loss lasted at least 30 days suggesting a relatively persistent effect. The data did not support the hypothesis that this level of hearing loss will decrease the density of PV, PNN and/or PV/PNN double-labeled cells in A1. However, a significant layer- and cell type-specific decrease in PNN intensity was seen in the noise-exposed groups. In superficial layers (I-IV), the decline was seen even at 1 day PE. In the deep layers, a recovery of PNN intensity was observed between 10 and 30 days PE. PNN cells with PV showed a decline in intensity only 30 days PE, whereas, PNN cells that did not express PV showed significant decline at 10 and 30 day PE. This suggests that PV may afford some degree of protection to PNN expression. We interpret the changes in PNN intensity to be driven by hearing loss. This interpretation has to be considered with the caveat that other areas in the cortex that are less likely to be affected by the noise trauma were not examined for PNN changes.

Considerable focus has been allocated to identifying the contributions of PNNs to developmental and adult plasticity. Strong evidence suggests that PNNs provide stability to the excitation-inhibition balance and adult plasticity can be promoted by breaking down PNNs (Takesian and Hensch, 2013; Happel et al., 2014). However, surprisingly little is known about the contribution of PNNs to the response properties of neurons they cover (Balmer, 2016). It is clear that cortical PNNs surround mostly GABAergic neurons with preference for PV+ neurons. This suggests that PNNs influence inhibition generated by fast spiking interneurons within cortical circuits. The differences between firing properties of cortical interneurons that are covered with PNN compared with those that are not remains unclear (Dityatev et al., 2007). A

recent study suggests that PNN increases excitability of fast-spiking, PV+ cortical cells (Balmer, 2016). Because cortical PV+ cells are mostly inhibitory, these data indicate that deterioration of PNNs may increase network excitability. A few studies have suggested that PNNs may provide protection against oxidative stress related cell death (Cabungcal et al., 2013) and also impact the expression of PV in GABAergic cells. This is again mainly relevant for fast spiking interneurons. Integrating available data from the literature, the present study makes the suggestion that acoustic trauma causes an attenuation of PNN intensity that opens up the circuitry for changes in excitation-inhibition balance. Such acoustic experience dependent changes in PNN intensity without a change in the density of PNN expressing cells have been previously reported in songbird vocal learning circuits (Balmer et al., 2009). Mature PNNs contain several CSPGs in addition to hyaluronan, tenascin-C and high amounts of tenascin-R, hyaluronan synthase and link proteins (Ctrl1). The reduction in PNN intensity may reflect changes in CSPG protein levels and composition and/or hyaluronan synthase and/or link protein levels.

Changes in inhibition following noise exposure may be one of the steps in causing an increase in gain and potentially, pathological activity (e.g., tinnitus). Evidence for such pathology correlated with changes in PNN comes from studies of epileptogenesis (Dityatev et al., 2010; McRae et al., 2012). Decline of PNN intensity in superficial layers even within 1 day PE suggests that this may be one of the first steps of cortical structural change. The recovery of PNN intensity to control levels at 30 day PE suggests the presence of a window following trauma during which circuit plasticity may occur and be stabilized at a new homeostatically adjusted level. However, future experiments that look at additional time points are needed to determine if there is a sustained recovery. The events leading up to the decline in PNN intensity may include changes to matrix metalloproteases (MMP) and cartilage link proteins (e.g., Ctrl1). MMP-9 is an

endopeptidase that cleaves extracellular matrix including PNN. MMP-9 levels are regulated by activity and high MMP-9 levels lead to increased breakdown of PNN. This suggests the hypothesis that MMP-9 levels increase within 1 day of noise exposure. This hypothesis remains to be tested. Carulli et al. (2010) showed that mice lacking Ctrl1, a PNN component, show attenuated PNNs including reduced intensity. The attenuated PNN promoted cortical plasticity in adults. Thus future studies of A1 following acoustic trauma should analyze expression levels of MMP-9 and Ctrl1 at specific time points after exposure.

Acknowledgements:

We thank the members of the Razak Lab for valuable inputs on the project and an earlier version of the manuscript.

Funding: This study was funded by UC, Riverside Academic Senate research grant.

**References:**

1. Anderson, L.A., Christianson, G.B., and Linden, J.F. (2009). Mouse auditory cortex differs from visual and somatosensory cortices in the laminar distribution of cytochrome oxidase and acetylcholinesterase. Brain Research 1252, 130–142. DOI: 10.1016/j.brainres.2008.11.037
2. Balmer, T.S. (2016). Perineuronal nets enhance the excitability of fast-spiking neurons. Eneuro ENEURO.0112–0116.2016. DOI: 10.1523/ENEURO.0112-16.2016
3. Balmer, T.S., Carels, V.M., Frisch, J.L., and Nick, T.A. (2009). Modulation of Perineuronal Nets and Parvalbumin with Developmental Song Learning. J. Neurosci. 29, 12878–12885. DOI: 10.1523/JNEUROSCI.2974-09.2009

4. Beebe, N.L., Young, J.W., Mellott, J.G., and Schofield, B.R. (2016). Extracellular Molecular Markers and Soma Size of Inhibitory Neurons: Evidence for Four Subtypes of GABAergic Cells in the Inferior Colliculus. J. Neurosci. 36, 3988–3999.
5. Berger, J.I., and Coomber, B. (2015). Tinnitus-Related Changes in the Inferior Colliculus. Front Neurol *6*. DOI: 10.3389/fneur.2015.00061
6. Brewton, D.H., Kokash, J., Jimenez, O., Pena, E.R., and Razak, K.A. (2016). Age-Related Deterioration of Perineuronal Nets in the Primary Auditory Cortex of Mice. Front. Aging Neurosci. 8. DOI: 10.3389/fnagi.2016.00270
7. Brückner, G., Seeger, G., Brauer, K., Härtig, W., Kacza, J., and Bigl, V. (1994). Cortical areas are revealed by distribution patterns of proteoglycan components and parvalbumin in the Mongolian gerbil and rat. Brain Research 658, 67–86. DOI: 10.1016/S0006-8993(09)90012-9
8. Cabungcal, J.-H., Steullet, P., Morishita, H., Kraftsik, R., Cuenod, M., Hensch, T.K., and Do, K.Q. (2013). Perineuronal nets protect fast-spiking interneurons against oxidative stress. Proc Natl Acad Sci U S A 110, 9130–9135. DOI: 10.1073/pnas.1300454110
9. Carulli, D., Pizzorusso, T., Kwok, J.C.F., Putignano, E., Poli, A., Forostyak, S., Andrews, M.R., Deepa, S.S., Glant, T.T., and Fawcett, J.W. (2010). Animals lacking link protein have attenuated perineuronal nets and persistent plasticity. Brain 133, 2331–2347. DOI: 10.1093/brain/awq145
10. Celio, M.R.(1993).Perineuronal nets of extracellular matrix around parvalbumin-containing neurons of the hippocampus. *Hippocampus* 3, 55–60.
11. Dityatev, A. (2010). Remodeling of extracellular matrix and epileptogenesis. Epilepsia 51, 61–65. DOI: 10.1111/j.1528-1167.2010.02612.x

12. Dityatev, A., Brückner, G., Dityateva, G., Grosche, J., Kleene, R., and Schachner, M. (2007). Activity-dependent formation and functions of chondroitin sulfate-rich extracellular matrix of perineuronal nets. Devel Neurobio 67, 570–588. DOI: 10.1002/dneu.20361.

13. Eggermont JJ (2015) Animal models of spontaneous activity in the healthy and impaired auditory system. Front Neural Circuits. 9:19. doi: 10.3389/fncir.**2015**.00019.

14. Enwright, J.F., Sanapala, S., Foglio, A., Berry, R., Fish, K.N., and Lewis, D.A. (2016). Reduced Labeling of Parvalbumin Neurons and Perineuronal Nets in the Dorsolateral Prefrontal Cortex of Subjects with Schizophrenia. Neuropsychopharmacology 41, 2206–2214. DOI: 10.1038/npp.2016.24

15. Fader, S.M., Imaizumi, K., Yanagawa, Y., and Lee, C.C. (2016). Wisteria Floribunda Agglutinin-Labeled Perineuronal Nets in the Mouse Inferior Colliculus, Thalamic Reticular Nucleus and Auditory Cortex. Brain Sci 6. DOI: 10.3390/brainsci6020013

16. Happel, M.F.K., Niekisch, H., Castiblanco Rivera, L.L., Ohl, F.W., Deliano, M., and Frischknecht, R. (2014). Enhanced cognitive flexibility in reversal learning induced by removal of the extracellular matrix in auditory cortex. Proc Natl Acad Sci U S A 111, 2800–2805. DOI: 10.1073/pnas.1310272111

17. Kosaka, T., and Heizmann, C.W. (1989). Selective staining of a population of parvalbumin-containing GABAergic neurons in the rat cerebral cortex by lectins with specific affinity for terminal N-acetylgalactosamine. Brain Research 483, 158–163. DOI: 10.1016/0006-8993(89)90048-6

18. Liu, H., Xu, H., Yu, T., Yao, J., Zhao, C., and Yin, Z.Q. (2013). Expression of Perineuronal Nets, Parvalbumin and Protein Tyrosine Phosphatase σ in the Rat Visual

Cortex During Development and After BFD. Current Eye Research 38, 1083–1094. DOI: 10.3109/02713683.2013.803287

19. Llano, D.A., Turner, J., and Caspary, D.M. (2012). Diminished cortical inhibition in an aging mouse model of chronic tinnitus. J Neurosci *32*, 16141–16148. DOI: 10.1523/JNEUROSCI.2499-12.2012.
20. Luo H, Pace E, Zhang J (2016) Blast-induced tinnitus and hyperactivity in the auditory cortex of rats. Neuroscience. pii: S0306-4522(16)30627-3. doi: 10.1016/j.neuroscience.2016.11.014.
21. Martin del Campo, H.N., Measor, K.R., and Razak, K.A. (2012). Parvalbumin immunoreactivity in the auditory cortex of a mouse model of presbycusis. Hearing Research 294, 31–39. DOI: 10.1016/j.heares.2012.08.017
22. McRae, P.A., Rocco, M.M., Kelly, G., Brumberg, J.C., and Matthews, R.T. (2007). Sensory Deprivation Alters Aggrecan and Perineuronal Net Expression in the Mouse Barrel Cortex. J. Neurosci. 27, 5405–5413. DOI: 10.1523/JNEUROSCI.5425-06.2007
23. McRae, P.A., Baranov, E., Rogers, S.L., and Porter, B.E. (2012). Persistent decrease in multiple components of the perineuronal net following status epilepticus. Eur J Neurosci 36, 3471–3482. DOI: 10.1111/j.1460-9568.2012.08268.x
24. Nakamura, M., Nakano, K., Morita, S., Nakashima, T., Oohira, A., and Miyata, S. (2009). Expression of chondroitin sulfate proteoglycans in barrel field of mouse and rat somatosensory cortex. Brain Research 1252, 117–129. DOI: 10.1016/j.brainres.2008.11.022

528 25. Novák, O., Zelenka, O., Hromádka, T., and Syka, J. (2016). Immediate manifestation of
529 acoustic trauma in the auditory cortex is layer specific and cell type dependent. Journal of
530 Neurophysiology *115*, 1860–1874. DOI: 10.1152/jn.00810.2015
531 26. Pantazopoulos, H., Lange, N., Hassinger, L., and Berretta, S. (2006). Subpopulations of
532 neurons expressing parvalbumin in the human amygdala. J. Comp. Neurol. *496*, 706–722.
533 DOI: 10.1002/cne.20961
534 27. Pilati, N., Ison, M.J., Barker, M., Mulheran, M., Large, C.H., Forsythe, I.D., Matthias, J.,
535 and Hamann, M. (2012). Mechanisms contributing to central excitability changes during
536 hearing loss. PNAS *109*, 8292–8297. DOI: 10.1073/pnas.1116981109
537 28. Pizzorusso, T., Medini, P., Berardi, N., Chierzi, S., Fawcett, J.W., and Maffei, L. (2002).
538 Reactivation of Ocular Dominance Plasticity in the Adult Visual Cortex. Science 298,
539 1248–1251. DOI: 10.1126/science.1072699
540 29. Roberts, L.E., Eggermont, J.J., Caspary, D.M., Shore, S.E., Melcher, J.R., and
541 Kaltenbach, J.A. (2010). Ringing Ears: The Neuroscience of Tinnitus. J. Neurosci. 30,
542 14972–14979. DOI: 10.1523/JNEUROSCI.4028-10.2010
543 30. Scholl, B., and Wehr, M. (2008). Disruption of Balanced Cortical Excitation and
544 Inhibition by Acoustic Trauma. Journal of Neurophysiology 100, 646–656. DOI:
545 10.1152/jn.90406.2008
546 31. Sonntag, M., Blosa, M., Schmidt, S., Rübsamen, R., and Morawski, M. (2015).
547 Perineuronal nets in the auditory system. Hearing Research 329, 21–32. DOI:
548 10.1016/j.heares.2014.12.012.
549 32. Syka, J., Rybalko, N., and Popelář, J. (1994). Enhancement of the auditory cortex evoked
550 responses in awake guinea pigs after noise exposure. Hearing Research 78, 158–168.

33. Syka J, Rybalko N. (2000) Threshold shifts and enhancement of cortical evoked responses after noise exposure in rats. Hear Res. 139:59-68.

34. Takesian, A.E., and Hensch, T.K. (2013). Balancing Plasticity/Stability Across Brain Development. In Progress in Brain Research, M.N. and T.M.V.V. Michael M. Merzenich, ed. (Elsevier), pp. 3–34.

35. Wang, H., Brozoski, T.J., and Caspary, D.M. (2011). Inhibitory neurotransmission in animal models of tinnitus: Maladaptive plasticity. Hearing Research *279*, 111–117.

36. Yamada, J., Ohgomori, T., and Jinno, S. (2015). Perineuronal nets affect parvalbumin expression in GABAergic neurons of the mouse hippocampus. Eur J Neurosci *41*, 368–378. DOI: 10.1111/ejn.12792.

37. Yang, S., Weiner, B.D., Zhang, L.S., Cho, S.-J., and Bao, S. (2011). Homeostatic plasticity drives tinnitus perception in an animal model. PNAS *108*, 14974–14979.

38. Yang S, Su W, Bao S (2012) Long-term, but not transient, threshold shifts alter the morphology and increase the excitability of cortical pyramidal neurons. J Neurophysiol. 108:1567-1574.

39. Zhou, X., Jen, P.H.-S., Seburn, K.L., Frankel, W.N., and Zheng, Q.Y. (2006). Auditory brainstem responses in 10 inbred strains of mice. Brain Res 1091, 16–26. DOI: 10.1016/j.brainres.2006.01.107

Figure Legends:

Figure 1. ABRs show that noise exposure caused considerable increase in hearing thresholds that lasted at least 30 days. (A) Example waveforms from a control mouse and (B) after 30 days following noise exposure. ABR thresholds were determined using sound level steps of 10 dB SPL. The hearing threshold for the control mouse in (A) was therefore noted to be between 30-40 dB SPL. The noise-exposed mouse (B) did not show any ABR up to 90 dB SPL (the highest level tested). (C-F) The hearing threshold of each mouse at specified time points is shown. The symbols within a sound level bin (ordinate) are jittered for visualization purposes. N=5 for each group. (C) The thresholds in control mice remain at <50 dB SPL throughout the course of 30 days. (D, E, F) Post exposure, the thresholds increased to >90 dB SPL (the highest level tested), indicating threshold shifts that lasted at least 30 days PE.

Figure 2. (A) Example photomicrograph of a coronal section through A1 stained for PV (red) and PNN (green) in a control mouse. The white rectangle indicates the 400 μm wide window in A1 within which PV, PNN and co-labeled cells were quantified from this image. This rectangle is reproduced in (B) which shows that PV and PNN stained cells are present at a higher density in layers IV-VI compared to layers I-III. The highest density of PNN staining was seen in layer IV in which a banded pattern of cellular and neuropil staining was observed. Arrows point to examples of different cell types that are then shown in C, D, E. (C) PV cell without PNN, (D) PNN cell without PV, and (E) PV/PNN co-localized cell.

596 Figure 3. Photomicrographs of PV and PNN expression in the experimental groups. Arrows
597 indicate the cells shown at a higher magnification in the insets: (A) 1 day PE, (B) 10 days PE,
598 (C) 30 days PE. (A1, B1, C1) PV without PNN. (A2, B2, C2) PNN without PV and (A3, B3, C3)
599 PV/PNN co-localized cells.
600
601
602 Figure 4. PV+ and PNN+ cell density in (A) layers I-VI, (B) layers I-IV and (C) layers V-VI
603 before and 1, 10 and 30 day PE. There was no statistically significant difference in the density of
604 stained cells following noise exposure.
605
606 Figure 5. Example photomicrographs from the control and experimental groups from which PNN
607 intensity was measured. Control (A) and 1 (B), 10 (C) and 30 (D) days after noise exposure.
608
609 Figure 6. Decline in PNN intensity in A1 following noise exposure. (A) In all layers combined,
610 there is a decrease in PNN intensity at 1 day PE and 10 days PE and a return to control levels at
611 30 day PE. (B) There is a decrease in PNN intensity in layers I-IV at 1 day PE, 10 days PE and
612 30 days PE compared to controls (C) There is a significant decrease in PNN intensity in layers
613 V-VI at 10 days PE followed by a significant increase by 30 days PE.
614
615 Figure 7. Examples to illustrate measurement of PNN intensity in the region around a cell. The
616 horizontal line centered on the PNN was 40 μm long. The bimodal graph shows the pixel
617 intensity along the horizontal line. The area under the curve can be used to measure PNN
618 intensity around cells. (A) Cell with a strong PNN label. (B) Cell with weak PNN staining.

Figure 8: Noise exposure caused a decline in PNN intensity in the region around cells in A1. (A) Average PNN intensity across all layers, (B) Average PNN intensity in layers I-IV (stripe bars) and layers V-VI (white bars) (*$p<0.05$, **$p<0.01$, ***$p<0.001$ for layers I-VI and $^{\#}p<0.05$ for layers V-VI). (C) PNN intensity in cells without PV (black bars) and with PV (gray bars) (*$p<0.05$, **$p<0.01$ for non-colocalized PNNs, $^{\#}p<0.05$ for co-localized PNNs).

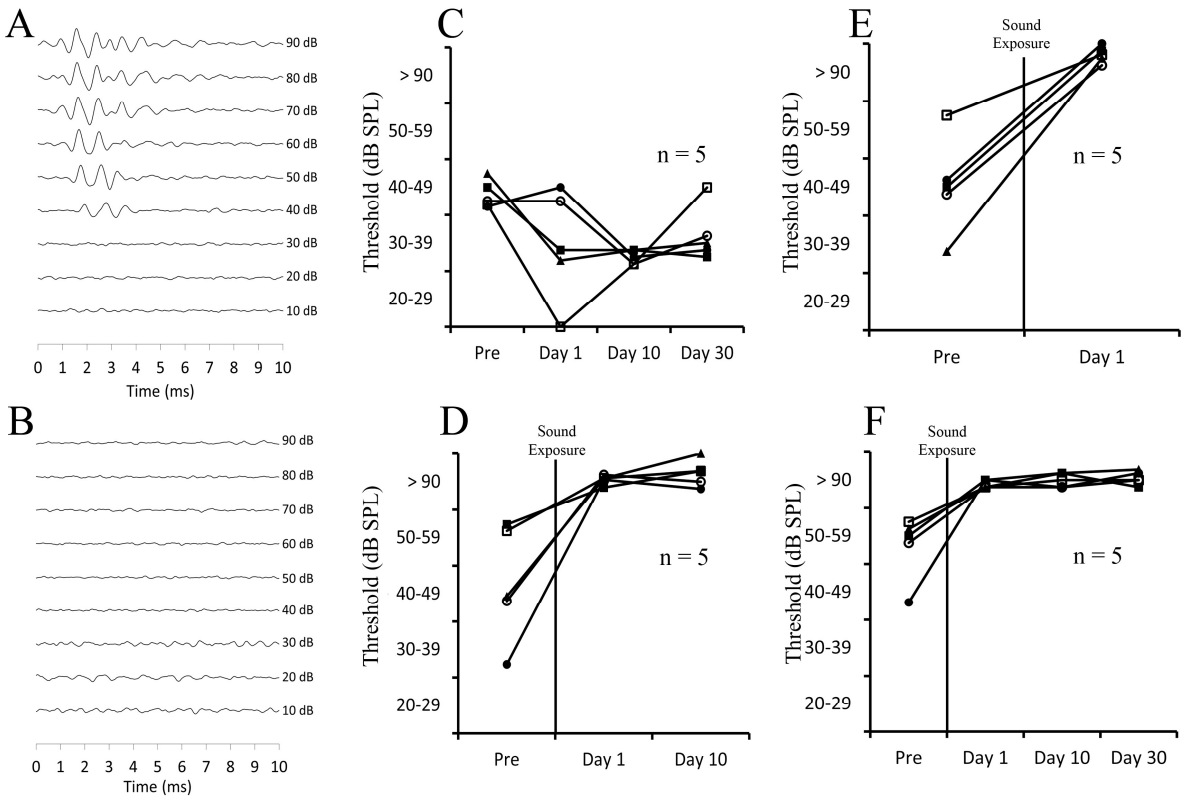

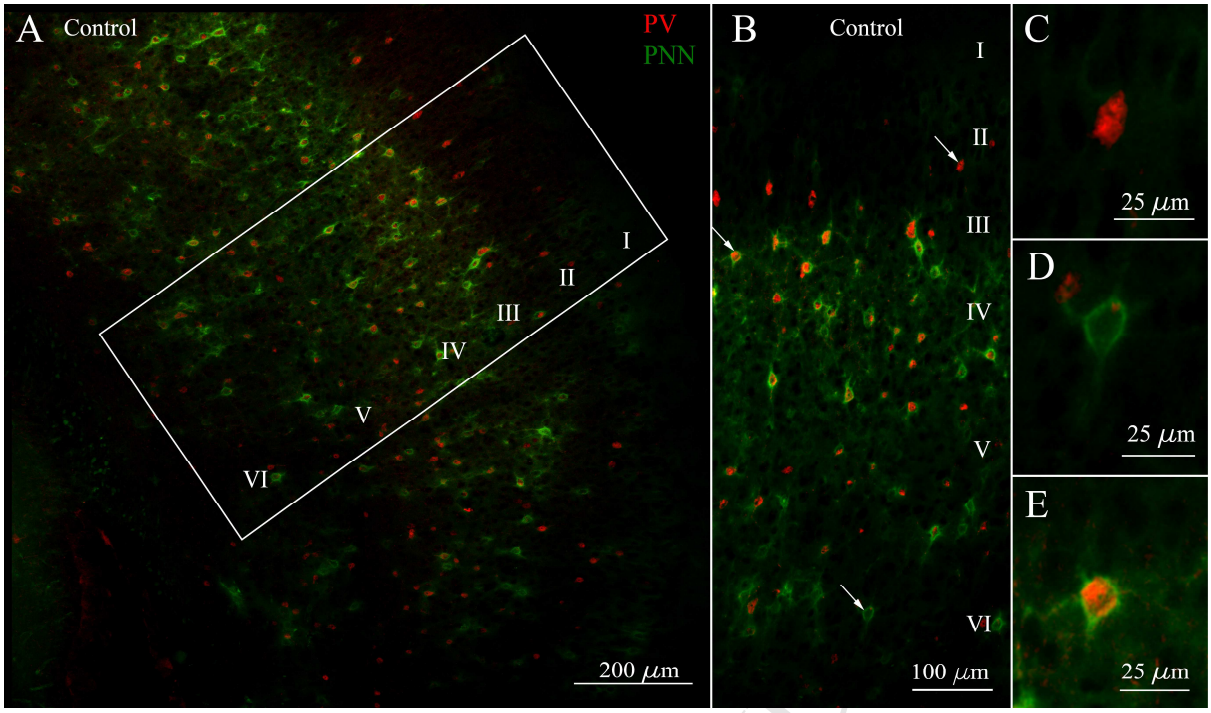

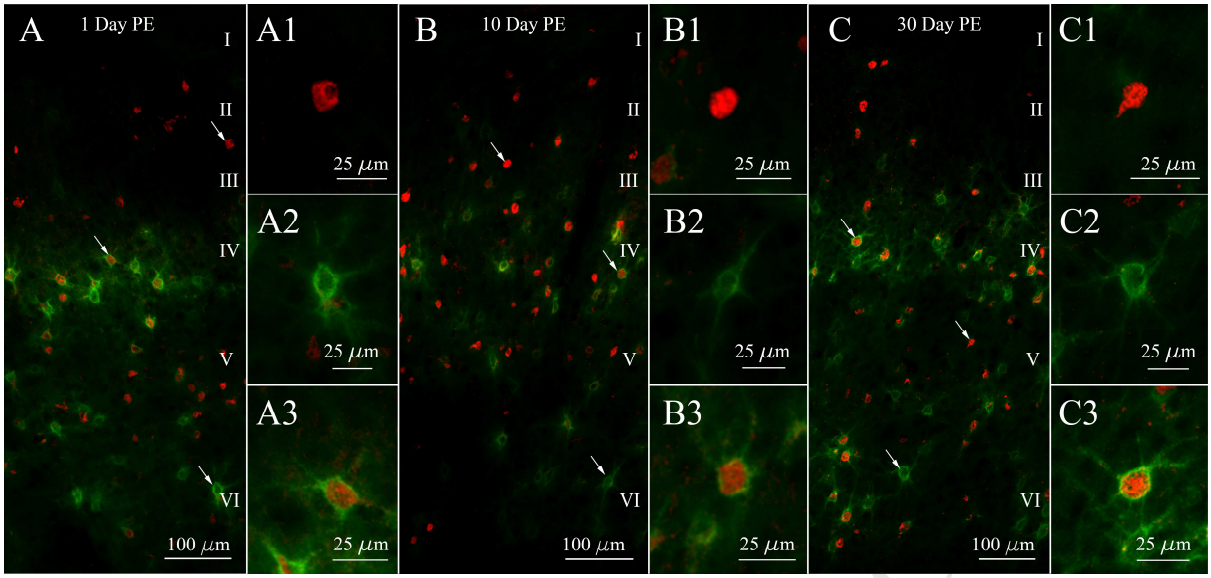

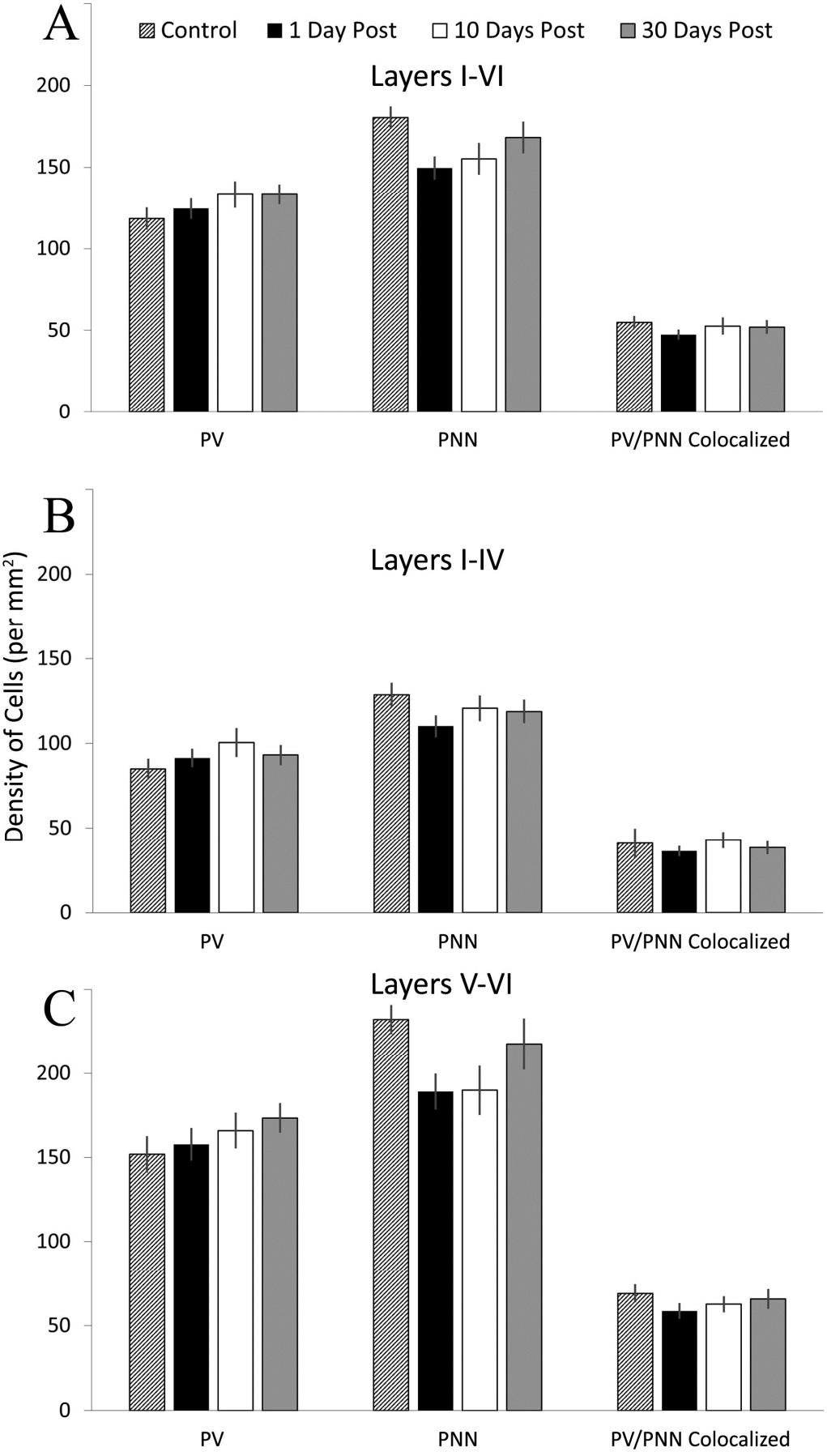
A
Control
1 Day Post
10 Days Post
30 Days Post
Layers I-VI
200
150
100
50
0
PV
PNN
PV/PNN Colocalized
B
Layers I-IV
Density of Cells (per mm²)
200
150
100
50
0
PV
PNN
PV/PNN Colocalized
C
Layers V-VI
200
150
100
50
0
PV
PNN
PV/PNN Colocalized

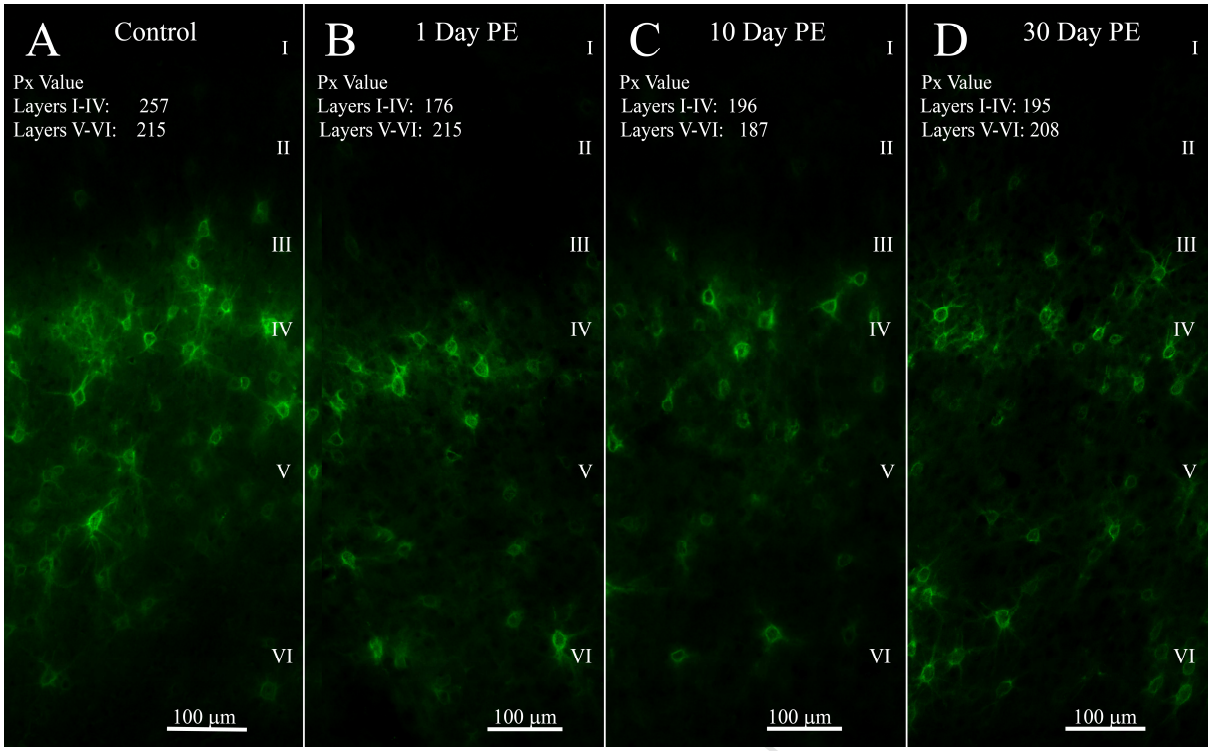

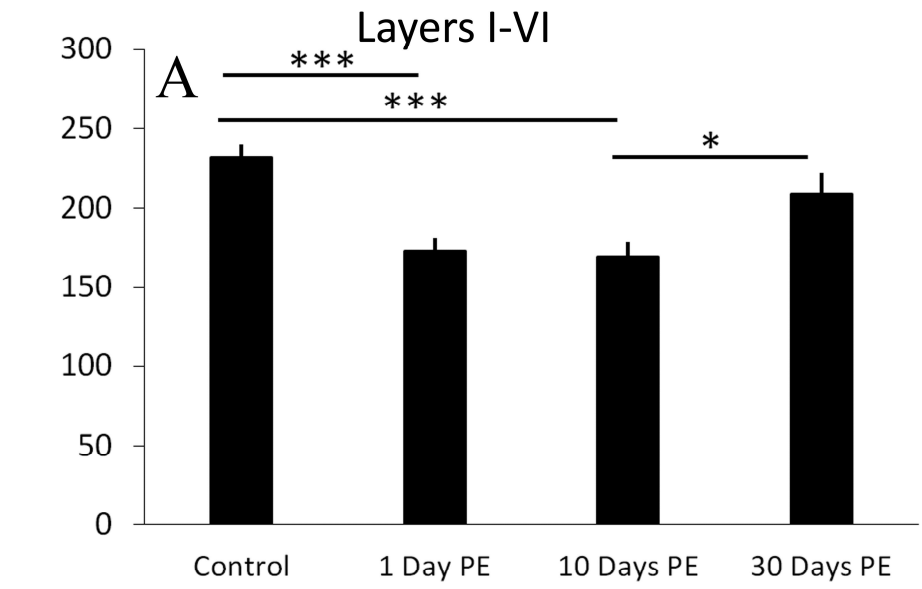
Layers I-VI
A
***
***
*
300
250
200
150
100
50
0
Control
1 Day PE
10 Days PE
30 Days PE

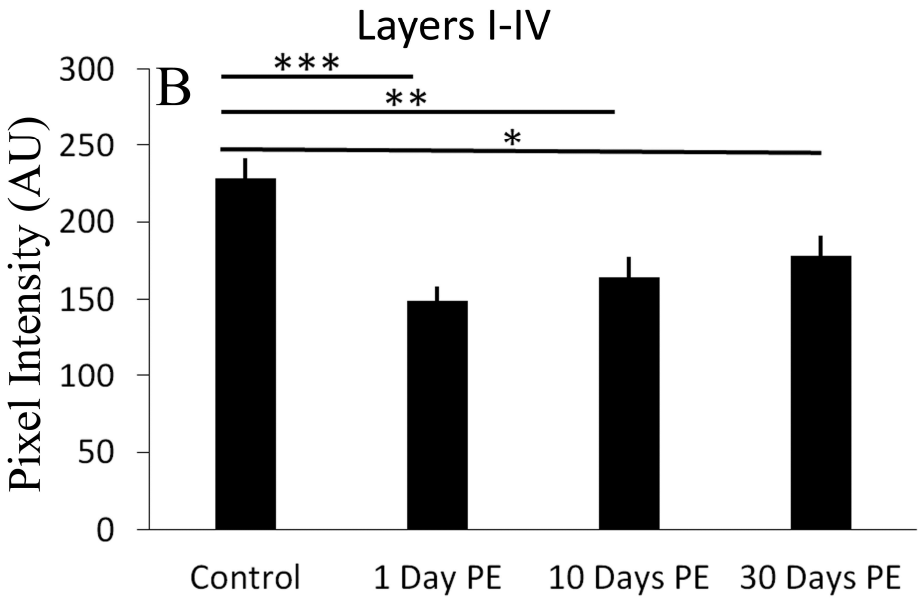
Layers I-IV
B
***
**
*
Pixel Intensity (AU)
300
250
200
150
100
50
0
Control
1 Day PE
10 Days PE
30 Days PE

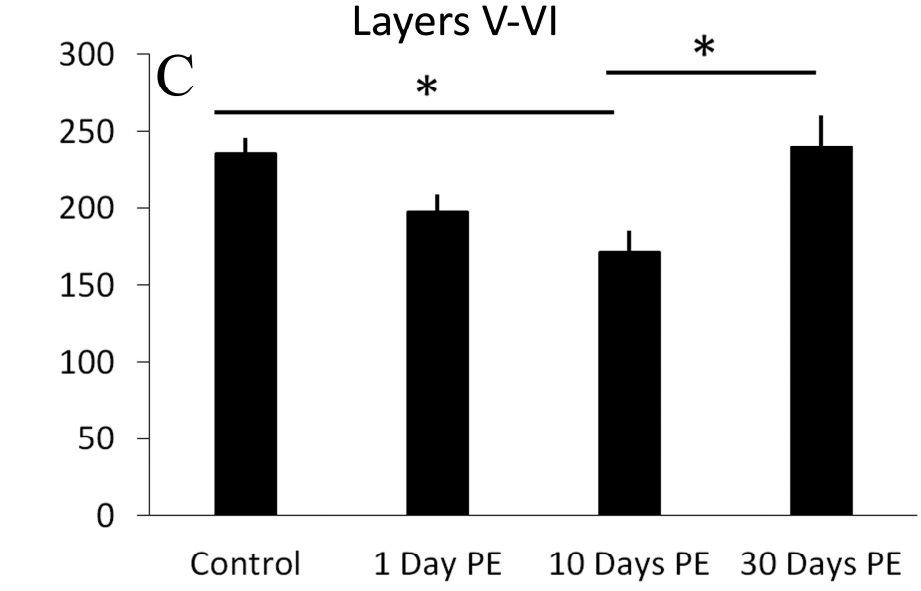
Layers V-VI
C
*
*
300
250
200
150
100
50
0
Control
1 Day PE
10 Days PE
30 Days PE

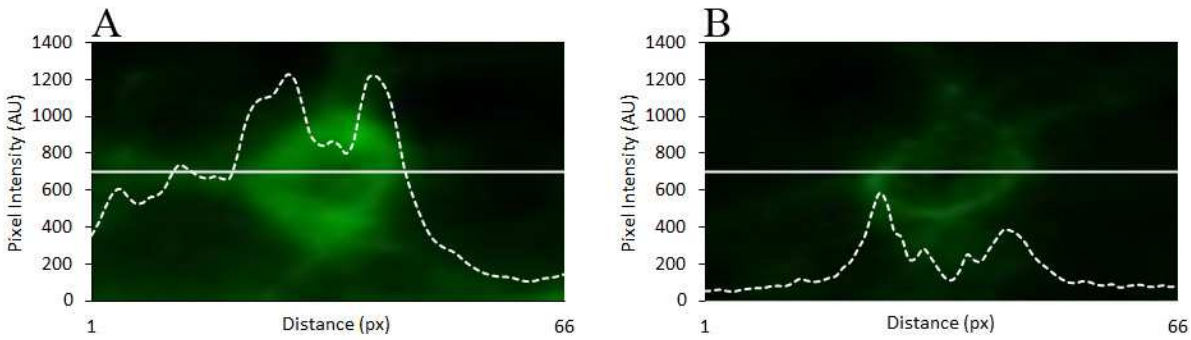

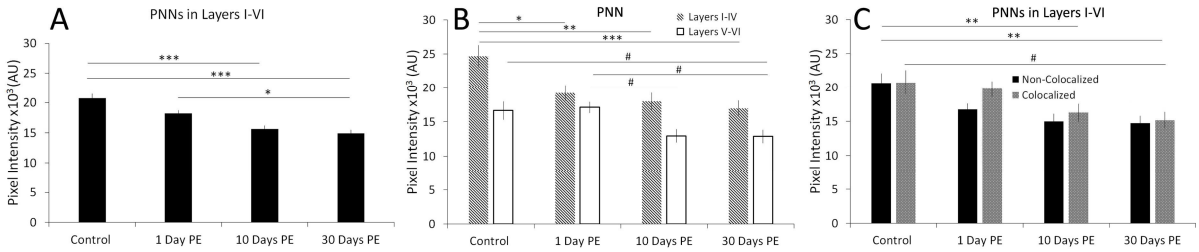

Highlights:

Acoustic trauma causes deterioration of perineuronal nets in auditory cortex

These changes show layer-specific trajectories following hearing loss induction

Decline of perineuronal nets is seen even at 1 day following noise exposure

Perineuronal net deterioration may cause increased excitability of auditory cortex